N O T I C E

THIS DOCUMENT HAS BEEN REPRODUCED FROM MICROFICHE. ALTHOUGH IT IS RECOGNIZED THAT CERTAIN PORTIONS ARE ILLEGIBLE, IT IS BEING RELEASED IN THE INTEREST OF MAKING AVAILABLE AS MUCH INFORMATION AS POSSIBLE

NASA Technical Memorandum 81491

OPTIMUM SUBSONIC, HIGH-ANGLE-OF-ATTACK NACELLES

Roger W. Luidens, Norbert O. Stockman,
and James H. Diedrich
Lewis Research Center
Cleveland, Ohio

Prepared for the
Twelfth Congress of the International Council of the Aeronautical Sciences
Munich, Germany, October 13-17, 1980
and the
1980 Aerospace Congress and Exposition
sponsored by the Society of Automotive Engineers
Los Angeles, California, October 13-16, 1980

OPTIMUM SUBSONIC, HIGH-ANGLE-OF-ATTACK NACELLES

by Roger W. Luidens, Norbert O. Stockman,
and James H. Diedrich

National Aeronautics and Space Administration
Lewis Research Center
Cleveland, Ohio 44135

ABSTRACT

Many proposed advanced aircraft - but especially tilt-nacelle, subsonic-cruise, V/STOL aircraft - require nacelles that operate over a wide range of aerodynamic conditions. The optimum design of such nacelles and their inlets is described, including how the inlet low-speed design conditions are selected, the conditions for which the various regions of the inlet are designed, and appropriate criteria of merit. For low-speed operation the optimum internal surface velocity distributions and skin friction distributions are described for three categories of inlets: those without boundary-layer control (BLC), those with BLC, and those with blow-in door slots and retractable slats. Experimental results are presented that show the performance of the various types of inlets. At cruise speed the effect of factors that reduce the nacelle external surface area and the local skin friction is illustrated. These factors are cruise Mach number, inlet throat size, fan-face Mach number, and nacelle contour. The interrelation of these cruise-speed factors with the design requirements for good low-speed performance is discussed. Finally an inlet design without BLC and an optimized inlet design with slots and slats are compared to illustrate the possible reductions in nacelle size.

INTRODUCTION

Many proposed advanced aircraft, especially subsonic V/STOL aircraft, require propulsion systems that operate over a wide range of aerodynamic conditions (fig. 1). The engine nacelle, and particularly the inlet, which must accommodate this wide range of conditions effectively and efficiently, is the subject of this report. The nacelle is more important for VTOL than for CTOL aircraft because the nacelle is relatively larger, because the engine thrust must be somewhat greater than the airplane weight, and because the range of required operating conditions is extremely wide.

At low speeds the inlet lower lip sees high angles of attack that may be due to such factors as a high airplane angle of attack, high wing upwash due to a high wing lift coefficient, or (for a tilt-nacelle airplane) a large nacelle tilt angle. The side lip is subject to cross winds from very large yaw angles. The top lip, which is not taxed by these other operating conditions, must still perform well at static conditions, especially for a VTOL aircraft in the vertical mode.

In the face of these adverse low-speed operating conditions the inlet must provide air to the engine at a high pressure recovery and low distortion. That is, the inlet internal flow should not separate.

At cruise conditions a low drag is desirable. This suggests a nacelle with a small surface area (i.e., a short, thin nacelle) and low skin friction coefficients. The best overall airplane performance will result for a lightweight nacelle, or again, a short, thin nacelle. The challenge then is to design a nacelle that meets all the requirements and yields the best possible airplane performance.

In recent years several V/STOL inlets without boundary-layer control[1,2] have been designed, primarily to meet the low-speed requirements. In the same time period there have been articles dealing with advanced concepts for inlets with good transonic maneuver capability[3] and for wings at high lift coefficients.[4,5] Some of these concepts seem applicable to subsonic inlets at high angles of attack. Boles[6] presents some experimentally observed diffusion flow limits for inlets. With these limits as background, Luidens[7] presents an approach to optimally designing an inlet without boundary-layer control that meets the low-speed requirements.

The present paper extends the approach to optimum inlet design presented by Luidens[7] to include the options for active and passive control of the boundary layer and expands the point of view to include the complete nacelle and the requirements for good cruise performance. The paper presents the concepts for optimum nacelle design and also some experimental results to support these ideas.

Finally, an example is given of the benefits gained from a boundary-layer-controlled, optimally designed nacelle. Although the present paper is particularly pertinent to V/STOL aircraft, which cruise at subsonic speeds, the overall approach to inlet and nacelle optimization is generally applicable.

SYMBOLS

A	flow area
A_f	area defined by fan blade tip
C_f	local skin friction coefficient (shear stress over local dynamic pressure)
CR	contraction ratio, $(r_h/r_t)^2$
M	Mach number
r	radius
S_w	surface area
s	surface distance
v	velocity
w	boundary-layer-control pump power
α	inlet flow angle of attack, deg
α_n	nacelle angle of attack, deg
δ	boundary-layer thickness
θ	circumferential position from windward meridian, deg

Subscripts:

bl	at the boundary-layer-control location
de	diffuser exit (fan face)
e	edge of boundary layer
f	fan
h	highlight
j	blowing jet
max	maximum value on surface
mc	main cowl
t	at throat
te	trailing edge of slat
0	free stream

DEFINITION OF PROBLEM

The general objective is to design a nacelle that will result in an aircraft design that will meet all the performance and mission requirements and yield an extremum in some aircraft criterion of merit, such as minimum gross weight. For the nacelle this involves several steps: (1) determining the operating conditions that set the design of each region of the nacelle, (2) specifying the constraints the nacelle design must meet, (3) selecting the design operating conditions, and (4) selecting a nacelle-related optimization criterion for choosing the best nacelle design. Each of these steps is discussed briefly.

Nacelle Regions

Three distinct low-speed flow conditions that control the design of three circumferential regions of the nacelle inlet are shown in figure 2. The most severe combination of approach velocity and flow angle of attack occurs for the bottom of the inlet. The flow angularity may be generated by airplane angle of attack, wing upwash, or (for a tilt-nacelle airplane) by the nacelle angle. For a tilt nacelle a typical difficult flow condition is a 60° flow angle at 120 knots. The next most difficult aerodynamic situation occurs on the side of the inlet, which must tolerate crosswinds of 35 knots at any yaw angle. The most difficult angle is about 120°. The top of the inlet is not a problem at the previously mentioned conditions. The inlet top is not subject to downward flow angularity, but it still must perform well at static conditions.

Cruise conditions influence the design of the inlet and of the entire external nacelle surface (fig. 2), particularly by the requirement of low cruise drag.

In general, the design conditions are different for the top and the bottom of the inlet, and so asymmetric designs can be anticipated. Because the bottom of the inlet has the most difficult requirements, the most attention will be given to it.

Design Constraints

There are some engine performance requirements that have implications for the inlet, such as (1) high engine thrust and efficiency; (2) low blade stresses; and (3) smooth, continuous thrust modulation. These constraints require high pressure recovery and low distortion, which in turn imply attached flow.

Initial Design-Point Selection

Proposed tilt-nacelle V/STOL aircraft concepts have very severe inlet design conditions, which will be used in the following discussions. However, the procedures described are applicable to other types of aircraft.

The wide range of flight conditions that can be encountered by a tilt-nacelle aircraft is illustrated in figure 1. Flight Mach number can vary from about 0.8 at cruise to zero at landing. Inlet angles of attack can be as high as 120°, and the range of engine throttle settings results in a wide range of throat (or fan face) Mach numbers. A combination of flight speed, nacelle angle, and throat Mach number constitute an inlet operating condition. It is not obvious from figure 1 what the worst, or design, condition is. A rational approach for defining the design condition is shown in figure 3.

Figure 3(a) considers the situation at a flight number of 0.18. The operating region is between 0° and 60° angle of attack for engine throttle settings that yield throat Mach numbers between 0.7 (full throttle) and 0.35 (part throttle). In this region, which is "blocked out" in the figure, attached flow is required. An inlet design should satify the requirement for attached flow in the operating region; a representative inlet separation bound is shown by the upper curve. The flow is attached everywhere below the curve. The point where the operating region and the inlet separation bound meet is the critical, or design, condition. In this case the design condition is in the low subsonic region, where compressibility effects are negligible. Therefore velocity ratios can be used instead of Mach numbers, as is done in figure 3(b).

Figure 3(b) now considers the situation all along the flight path in terms of angle of attack as a function of throat-to-free-stream velocity ratio v_t/v_0. The area labeled "operating region" now encompasses areas such as those from figure 3(a) for all free-stream Mach numbers. The inlet separation characteristic for a given subsonic inlet flow with $M_t < 0.6$ generally is normalized by the parameters of figure 3(b). The tangent point of the inlet operating region with the inlet separation bound curve is again the critical, or design, condition, but this time for the whole flight path. The example shown is for the case where point A is the same point in both figures 3(a) and (b).

The design process is actually an iterative one. After an inlet is designed, it must be determined if the design point has changed. This process is discussed in the section Review of Inlet Design-Point Selection.

Criteria of Merit

The general objective is to achieve a low airplane takeoff gross weight for a specified mission. The criterion to meet this objective is a lightweight and low-cruise-drag inlet, that is, a thin, short inlet. Note that low cruise drag means low friction drag, avoidance of external shock losses, avoidance of external flow separation, and recovery of additive drag by inlet lip thrust.

INLET OPTIMIZATION FOR LOW SPEEDS

This section discusses the optimum design of three categories of inlets, namely, (1) those without boundary-layer control (BLC), (2) those with BLC, and (3) those with boundary-layer management (BLM). Then some experimental results for these inlet categories are presented.

Designs Without Boundary-Layer Control

The discussion covers optimum flow distributions in inlets, empirical flow limits, and inlet geometry.

Optimum Flow Distribution - Flow distributions, that is, surface velocities and skin friction coefficients, for an optimum inlet design are described by Luidens[7] and are shown in figure 4. The velocity (fig. 4(a)) increases from zero at the stagnation point to a maximum flat-top value on the lip and then decelerates in the diffuser to the value required at the fan face or the diffuser exit.

The maximum velocity is as high as is allowable. The corresponding low static pressure acting on the lip surface area provides the suction force required to turn the high-angle-of-attack flow into the inlet. The lower the surface pressure, the shorter the lip surface distance can be. Both the flat top and the high level of velocity contribute to a shorter surface distance and hence a thinner lip. After the lip the velocity decelerates in the manner prescribed for a short, efficient diffuser.

The skin friction coefficient distribution corresponding to the velocity distribution of figure 4(a) is shown in figure 4(b). The boundary layer is initially laminar (ℓ), and it transitions (tr) to turbulent flow (t) by the end of the flat-top region and before it is subject to the rapid diffusion. Modifying the flat-top velocity to a slightly decreasing velocity will encourage the desired transition. In an ideal optimum diffuser the skin friction coefficient drops to zero to achieve the shortest, lowest loss diffusion. In a practical optimum diffuser a friction coefficient margin would be specified at the end of the diffusion, and a negative friction coefficient slope (fig. 4(b)) would be specified to ensure that, if separation did inadvertently occur, it would occur at the end of the diffuser and not at the middle or beginning of the diffuser.

Empirical Flow Limits - In general, a most important factor in determining the inlet lip thickness is the peak velocity allowable on the lip. Two parameters that limit the maximum allowable lip velocity are identified by Boles.[6] Both parameters define the onset of flow separation. They are called the Mach number limit and the diffusion limit. The Mach number limit is associated with an extremely rapid initial surface velocity deceleration or shock-boundary-layer interaction which causes separation near the beginning of the diffuser. The diffusion limit is related to the surface velocity deceleration from the peak velocity to the diffuser exit velocity v_{max}/v_{de}. Separation starts near the diffuser exit. If the separation is unstable, it then travels immediately to the lip. These two limits were determined empirically by plotting their experimental values just before separation against the throat-to-free-stream Mach number ratio, as shown in figure 5. Data are shown for several inlets and a range of operating conditions.

In figure 5(a) it can be seen that, as the throat-to-free-stream Mach number ratio M_t/M_0 increases, the peak Mach number increases and then levels off at about $M = 1.5$. Thus $M = 1.5$ is taken as the Mach number limit, and flow separation can be expected for local surface Mach numbers greater than 1.5.

In figure 5(b) the same data are replotted by using the diffusion ratio v_{max}/v_{de} as the ordinate. Now as M_t/M_0 decreases, the diffusion ratio increases to a limit and then decreases slightly. This limit is a function of contraction ratio and Reynolds number but in general falls in a band indicated as the diffusion limit in figure 5(b). For simplicity a constant value of 2.5 will be taken as the diffusion limit, and flow separation can be expected for higher values. Stratford[8] has predicted a theoretical limiting diffusion ratio of about 3.2, which is consistent with these experimental results.

The values of $M_{max} = 1.5$ and $v_{max}/v_{de} = 2.5$ will be used in the following discussion. In a refined analysis the secondary effects evident in the experimental data could be accounted for in an iterative procedure starting with values we have selected.

Inlet Geometry - The shortest, thinnest inlet with attached inlet flow will result when the inlet geometry is designed for the optimum surface velocity and skin friction distributions and designed to the flow limits of diffusion velocity and Mach number just discussed. Appropriate allowances may be made for a safety margin and separation stability.

The approach is then to find the lip shape and thickness and the diffuser shape and length that yield the required flow distributions and limits. This can be done by systematic geometric changes[9] using the potential and viscous flow calculational procedures of Stockman.[10]

If each circumferential region of the inlet is designed to meet only its requirement, then because the requirements vary around the circumference of the lip, the design will also vary around the circumference. So, in general, asymmetric geometries result. Figure 6 shows two asymmetric inlet designs.

Thick Lower Lip - The inlet shown in figure 6(a) is characterized by an inlet highlight plane normal to the inlet axis. The inlet lip thickness varies around the circumference in order to satisfy the angle-of-attack requirement on the bottom, the cross-wind requirement on the side, and the static performance requirement on the top. The relative difficulty of these requirements is reflected in the lip thickness. Clearly the lower lip has the most difficult requirement.

Protruding Lower Lip - Another approach to meeting the lower lip requirement, besides thickening it, is to extend it as shown in figure

6(b). At low speeds and zero angle of attack, the protruding lower lip causes the inlet to draw its air generally from above the inlet axis. Compared with a conventional inlet this increases the peak surface velocity on the upper lip and reduces it on the lower lip. The effect of angle of attack is to increase the peak surface velocity on the lower lip (and decrease it on the upper lip). Because the lower lip velocity at zero angle of attack is low, the inlet can go to a high angle of attack before the peak lower lip velocity causes the diffusion velocity ratio limit to be exceeded.

The static and cruise conditions require special attention for this inlet.

Designs with Boundary-Layer Control

The optimum surface velocity distributions and the experimentally observed flow limits without boundary-layer control (BLC) have been discussed. Consider next the surface velocity distribution with BLC. The object of using BLC is to achieve a thinner inlet for specified operating conditions by increasing the permissible maximum velocity.

Optimum Flow Distribution - Three velocity distributions are presented in figure 7. Figure 7(a) is the optimum distribution without BLC, the case previously discussed, and it has a maximum velocity ratio v_{max}/v_{de} of 2.5. For the selected design flow conditions this yields a thick lip, as shown by the sketch under the velocity profile. Figure 7(b) presents the optimum velocity distribution for the optimum location of a point application of BLC. The maximum velocity ratio v_{max}/v_{de} is now 6.25 (2.5^2), as explained later. The flow accelerates from the stagnation point, $v = 0$, to the flat-top velocity ratio of 6.25. After the flat top it decelerates through a velocity ratio v_{max}/v_{bl} of 2.5, that is, from $v_{max}/v_{de} = 6.25$ to $v_{bl}/v_{de} = 2.5$. Here, the boundary layer is on the verge of separation. It is now either completely removed or completely reenergized so that it can just diffuse through the remaining velocity ratio of $v_{bl}/v_{de} = 2.5$, that is, to $v/v_{de} = 1.0$ at the diffuser exit. This high peak velocity results in a very thin lip, as shown by the sketch under this velocity profile. The flow is on the verge of separation at the BLC site and at the diffuser exit.

An intermediate case is shown in figure 7(c). The flat-top velocity ratio is taken as $v_{max}/v_{de} = 5.0$. Now there are two limiting choices. The flow can be diffused from the peak through a velocity ratio of 2.5 to point A, and BLC applied. The remaining diffusion ratio is a conservative value of 2.0. Or the flow can be diffused from the peak through a conservative velocity ratio of 2.0 to point B, and BLC applied. The remaining diffusion is now at the limiting value of 2.5. Actually, the BLC can be applied anywhere between points A and B and the flow will be within the diffusion limit. The lip thickness for this case is intermediate between those of the two preceding cases.

If the design condition is inadvertently exceeded and flow separation occurs, it would be preferable for the separation to occur at the diffuser exit rather than at the BLC site. From this point of view a BLC site at B is preferable. Thus far, the type of BLC has not been specified. Next, three kinds of BLC are considered: suction, blowing, and self pumping.

Suction. - An idealized suction (also called bleeding) BLC system together with its nomenclature is shown in figure 8(a). The figure shows the boundary layer, the suction surface, and the pumping system required to pump the bleed air back to free-stream conditions.

The inlet flow starts from the stagnation point, first accelerating and then diffusing, and before separation proceeds to a downstream point bl, where the suction starts. The suction system removes the minimum possible amount of the boundary layer consistent with keeping the flow attached. Conceptually, the suction can be distributed downstream of station bl or concentrated at that station. Of course, the diffusion continues from station bl to the diffuser exit, station de.

There are two important streamlines: One is through the edge of the boundary layer at station bl. The other is the dividing streamline, labeled div, which divides the flow that is removed from the rest of the flow. The flow not removed must undergo the required diffusion from v_{bl} to v_{de}. The boundary layer removed is assumed to be drawn into a plenum chamber whose static pressure is equal to that at the beginning of the suction region and to have no residual velocity head. From there it is sent through a pump to raise the pressure back to free-stream total pressure and ducted overboard to ambient pressure and in the downstream direction, resulting in no thrust or drag.

The power to drive the pump, which is discussed shortly, is a function of the diffuser exit Mach number, the diffusion velocity ratio from the start of the suction to the diffuser exit v_{bl}/v_{de}, and the boundary-layer profile.

Blowing. - An idealized blowing boundary-layer-control system together with its nomenclature is shown in figure 8(b) and is quite similar to the suction case just discussed (fig. 8(a)). Whereas in the suction case that portion of the boundary-layer flow that does not have sufficient momentum to negotiate the subsequent diffusion is removed, in the blowing case it is reenergized by the blowing jet. In this case the dividing streamline divides the boundary-layer flow that is reenergized from that which is not. It is assumed that the blowing jet and that portion of the boundary layer to be reenergized mix immediately to produce a uniform velocity (station bl after mixing) that is just sufficient to diffuse to zero velocity at the diffuser exit (station de).

The power to drive the blowing system pump depends on the same parameters as the power for the suction system, plus the additional parameter of the jet-to-boundary-layer-edge velocity ratio v_j/v_{bl}.

The relative power required by the pumps for BLC is shown in figure 9 as a function of the ratio of the velocity at the BLC site to that at

the diffuser exit v_{bl}/v_{de}. This ratio defines the location of the BLC, with larger values corresponding to more upstream locations. The analysis is limited to, and the curves terminate at, the diffusion limit, $v_{bl}/v_{de} = 2.5$. The following conditions were specified for figure 9: a diffuser exit Mach number M_{de} of 0.3 and a 1/7-power boundary-layer velocity profile.

For the present flow models, suction requires more power than blowing. The reason for this is associated with the loss of the boundary-layer momentum removed through the suction surface. In general, BLC requires the least power if it is done at the lowest velocity v_{bl}, that is, for example, at point A in figure 7(c). The disadvantage of this location as suggested earlier is that, should the design condition be inadvertently exceeded, separation will first occur about midway up the diffuser at point A and this results in an undesirable large separation region ahead of the fan. A more tolerable location for initial separation is near the diffuser exit. This can be achieved by moving the BLC upstream to point B, where v_{bl} is higher. However, now the pump power is also higher. In general, a safety margin is achieved at the expense of power.

Self Pumping - The preceding analysis dealt with a suction system for which the air removed was pumped back up to free-stream total pressure and then exhausted overboard. In that case the power to drive the pump is significant and is a measure of the penalty associated with the system. The sketch in figure 10 shows a self-pumping suction system.[11]

Recall that separation occurs on the windward side of the inlet and usually in the diffuser. The suction slot is located in this region and has, for example, a circumferential extent θ of $\pm 45^\circ$ about the windward, or 0°, meridian. The reinjection holes are located on the lip and are displaced circumferentially from the suction slot in order to avoid recirculation of the boundary layer from the reinjection holes to the suction slot. For example, the reinjection holes extend, on each side of the inlet, between 45° and 60°. The suction slot and the reinjection holes are connected by a circumferential plenum.

The locations of the suction slot and reinjection holes are based on the theoretical surface static-pressure distribution shown in figure 10 for an inlet at high angle of attack. In general, for a given value of θ, the pressures are lowest on the lip and increase through the diffuser to the fan face. Also, for a given axial location the pressures are lowest at a θ of 0° and increase with increasing θ. The large pressure difference from the lip to the diffuser exit at 0° is, of course, what makes 0° critical with respect to flow separation. Thus the boundary-layer-control slot is centered about $\theta = 0^\circ$. For this bleed system to work, the static pressure must be lower at the reinjection holes than at the suction slot. Thus it is helpful to have the axial location of the suction slot well into the diffusion region, where the static pressures are higher. As mentioned previously, to avoid recirculation into the suction slot, the reinjection holes must be displaced circumferentially from the suction slot, for this example at $\theta > 45^\circ$. To be at a lower surface static pressure the reinjection holes must be upstream of the suction slot. The circumferential extent of the reinjection holes is limited by the increase in static pressure with increasing θ and the related reduction of the static-pressure gradient between the suction slot and the reinjection holes.

The minimum pressure at reinjection holes below a θ of 90° decreases with increasing angle of attack, and correspondingly the suction at the suction slot increases. This tends to make the system self-activating and controlling. Miller[11] shows that this bleed system can indeed be made to work. This system avoids the need for an external source of power or air.

Designs with Boundary-Layer Management

The preceding section dealt with methods to reenergize or remove a boundary layer that is not capable of further diffusion. Another way of accomplishing the desired further diffusion is starting a new boundary layer, for example, by means of a slat. This starting of a new boundary layer, called boundary-layer management (BLM), is dicussed in this section.

Optimum Flow Distribution - The inlet geometry, surface velocity distributions, and boundary-layer velocity profiles for this case are shown in figure 11. The basic geometry consists of a main cowl and a slat that can be formed by the translation forward of a portion of the main cowl or by blow-in doors that open a passage (called a slot) between the slat and the main cowl. The goal is to achieve a very high flat-top velocity distribution (e.g., a diffusion ratio of 6.25) and to avoid separation. This is accomplished by designing for a diffusion ratio of 2.5 on the slat and then another diffusion ratio of 2.5 on the main cowl ($6.25 = 2.5^2$). In this type of design three types of flow breakdown must be avoided: (1) separation of the boundary layer on the slat, (2) flow reversal in the slat wake downstream of the slat, and (3) separation of the main-cowl boundary layer. Each of these is considered in this section.

A high flat-top velocity profile on the slat at the design flow conditions can be achieved by proper contouring of the slat. A value of $v_{max}/v_{de} = 6.25$ is illustrated on the upper part of figure 11. Since a diffusion velocity ratio of 2.5 is the maximum tolerable value, the slat terminates when $v_{max}/v_{te} = 2.5$. The diffusion velocity ratio remaining, v_{mc}/v_{de}, is also 2.5. The velocity ratio of $v_{mc}/v_{de} = 2.5$ at the trailing edge of the slat is achieved by proper contouring of the main cowl as well as by the contouring of the slat. Thus the slat is performing at its limit with separation just avoided.

At the trailing edge of the slat the upper and lower surface boundary layers merge to form a wake. The flow in this low-energy wake could reverse (or separate within itself) if it is subject to too steep an adverse pressure gradient. To allow distance for the wake to mix with the surrounding high-energy air before it is diffused, a constant-velocity (and hence a constant static pressure) run is designed to occur down-

stream of the slat trailing edge, as illustrated in figure 11. The constant-velocity run is achieved by appropriate local contouring of the main cowl. The flow is, by definition, optimally mixed when it can just withstand the remaining diffusion (i.e., when $v_{mc}/v_{de} = 2.5$).

Like the slat wake the "new" boundary layer on the main cowl entering through the slot is also subject to the maximum tolerable diffusion ratio of $v_{mc}/v_{de} = 2.5$.

Two other general rules should be applied to the slat:

(1) The gap should be large enough so that the slat and main-cowl boundary layers do not merge.

(2) The slot passage should converge to the slat trailing edge (i.e., the passage minimum area should occur at the slat trailing edge).

The preceding discussion has dealt with a diffusion-limited design, that is, $M_{de} \leq 0.24$ for $v_{max}/v_{de} = 6.25$. If M_{de} is greater than 0.24, M_{max} will be greater than the limit of 1.5 and the flow on the slat will separate from compressibility effects. To avoid this type of separation, v_{max} on the slat must be lowered to achieve an M_{max} of 1.5. Thus for $M_{de} > 0.24$, the slat is Mach number limited and the main cowl is still diffusion limited.

If the diffusion exit Mach number M_{de} exceeds 0.6, the maximum Mach number on the main cowl will also exceed 1.5 for $v_{mc}/v_{de} = 2.5$, and the main cowl will also become Mach number limited. The surface Mach number distribution for this last case is shown by the inset in figure 11.

The application of boundary-layer management is illustrated for two inlets in figure 12.

Retractable Slat - The retractable-slat approach to an inlet design is shown in figure 12(a). The basic inlet is taken to be axisymmetric. The desired slat is achieved by moving a 120° segment of the windward lip forward and down, as illustrated. This has a number of beneficial aerodynamic effects, some of which are (1) that it provides the boundary-layer-management function just described, (2) that it increases the frontal area or contraction ratio of the critical lower lip, and (3) that it creates some lower lip protrusion. The increase in frontal area is especially important for inlets that are on the verge of separation because of the Mach number limit.

This slat requires mechanical actuation and is analogous to a wing leading-edge flap.

Slotted Inlet - The slotted-inlet approach is shown in figure 12(b). The basic inlet is again axisymmetric. In this case the slat is fixed relative to the main cowl and encompasses the entire circumference. The desired gap (slot) is formed when the blow-in doors (dashed lines), which are hinged at their downstream edge, move inward. This arrangement yields two aerodynamic benefits: (1) it provides the boundary layer management, and (2) it increases the inflow area. The aerodynamic forces on the inlet are such that the blow-in doors open automatically at low forward speeds and close automatically at high speeds.

Experimental Results

Most of the inlet concepts discussed herein have been tested, and the test results are summarized in figure 13. The angle of attack at which the inlet flow first separates is plotted against inlet lip contraction ratio CR, or lip thickness. In this coordinate system the most desirable characteristics are the lowest contraction ratio and the highest separation angle, that is, the upper left corner of the figure.

Consider first the inlet without boundary-layer control. The solid line shows that increasing the lip thickness does indeed increase the angle of attack for lip separation,[12,13] sketch A. However, this increased lip thickness is moving away from the stated goal of short, thin inlets. Protruding the lower lip of a modest-contraction-ratio lip is far more effective than thickening it,[14] sketch B. The protruding-lip inlet has static and cruise characteristics that need further study.

Active boundary-layer control achieved by blowing near the throat of the inlet also gives excellent performance,[15,16] sketch C. The data point shown was obtained with a blowing pressure ratio of 1.4. Additional performance gains are possible at higher blowing pressure ratios.

Three boundary-layer-management inlets were tested. A 120° lower lip slat was added to an inlet with a modest contraction ratio, and a marked increase in separation angle was obtained, sketch D. Next a very short inlet with a low contraction ratio but with a 360° slot was tested. It gave the performance shown at sketch E. Finally the slat used with configuration D was combined with configuration E to give the results at sketch F. This is the shortest, thinnest inlet with high-angle-of-attack capability thus far obtained.

In general, applying advanced design features can markedly improve inlet low-speed performance. These changes will also affect the inlet separation bound and may consequently affect the initial inlet design condition. Therefore inlet design-point selection will be reviewed in the next section.

Review of Inlet Design-Point Selection

Recall that the initial process of selecting an inlet design point (fig. 3) depended on knowing or estimating an inlet separation curve. The design point was found to be a low subsonic inlet flow condition. The preceding analysis and data showed that boundary-layer control or management schemes have a very strong effect on reducing the inlet lip thickness required to avoid flow separation, resulting in different separation bounds.

The overall design process is an iterative one, requiring that the new separation bounds be compared with inlet operating requirements to determine if the inlet design point has changed.

This process is illustrated in figure 14, which is a reproduction of figure 3 but with new separation characteristic curves, the solid lines, added. The lower solid line is for a slotted inlet with a low contraction ratio (fig. 13). It meets the requirements of the initial design point, point A in figure 14. However, the separation characteristic is not satisfactory at the higher operating throat Mach number, point B. This is because for low-contraction-ratio (e.g., CR < 1.3) inlets, the local surface Mach number rises to very high values (i.e., greater than 1.5) as the throat Mach number increases from point A. Thus point B becomes the new design point because it is the most difficult operating condition to meet.

As shown in the following section, achieving a low contraction ratio, like 1.2, at cruise is very desirable. However, design point B requires a larger contraction ratio. These conflicting requirements can be met by adding a retractable slat (fig. 13) to the low-CR slotted inlet. This slat is extended at low speeds but retracted at cruise speeds. A retractable slat that yields an effective lower lip contraction ratio of about 1.5 will satisfy the entire operating requirement and yield a low contraction ratio at cruise.

Nacelle Optimization for Cruise

In this section the effect of cruise conditions on the nacelle length and diameter is discussed. The factors to be considered are the free-stream (cruise) Mach number, the inlet throat size, the fan-face Mach number, and the nacelle external profile.

Cruise Mach Number - Figure 15 shows three nacelles designed by consistent rules and drawn to scale. The left two nacelles illustrate the effect of cruise Mach number. A characteristic feature of cruise is that the capture stream tube is smaller than the fan. The higher the cruise Mach number, the smaller the capture stream tube. Compare the upper figure for $M_0 = 0.9$ with the lower one for $M_0 = 0.75$.

A key design constraint is that the maximum local surface Mach number on the outside of the nacelle not exceed about 1.4 to avoid wave drag. This constraint is important for the following reason: The integral of the static pressures (actually $p - p_0$) on the outside of the capture stream tube up to the stagnation point produces a force in the free-stream direction termed the "additive drag." For a low nacelle drag this drag must be exactly offset by a "leading-edge suction" that results from lower than ambient pressures on the external lip. The minimum lip static pressure is set by M_{max}, which is why this constraint is important.

By decreasing the highlight area A_{hl} we can reduce the projected frontal area of the external surface of the capture stream tube that is generating the additive drag and increase the lip frontal area that generates the leading-edge suction. The penalty for decreasing the highlight area (and consequently decreasing throat area for a given contraction ratio) is an increase in inlet length for a given limit on the diffuser maximum wall angle and the diffuser wall shape. The nacelle design for $M_0 = 0.9$ that accounts for all these factors has an external-surface-to-fan-face frontal area ratio S_w/A_f of 10.

As shown in the lower left sketch in figure 15, if we reduce the cruise Mach number from 0.9 to 0.75, the capture stream tube is larger. The inlet length, as determined by the diffuser wall angle limit, is reduced. With the same nacelle design rules the external surface area can be reduced to an S_w/A_f of 6.7. Thus reducing the cruise Mach number reduces the nacelle size.

Inlet Throat Size - Another approach to designing a $M_0 = 0.75$ nacelle is shown in the lower right sketch in figure 15. The throat area of the nacelle is increased to equal the fan area, so the diffuser is eliminated. This shortens the inlet. The spillage frontal area, which generates the additive drag, has now increased. To compensate for this, the nacelle maximum diameter may be increased (while still maintaining a peak surface Mach number of 1.4), so the frontal area for leading-edge suction is also increased. Also, to mitigate the effect of increasing the throat area, the inlet contraction ratio A_h/A_t is reduced to 1.2. For this reduced contraction to be satisfactory at low speeds, a slot and a slat (previously discussed) must be used. At cruise speeds the slot is closed and the slat is retracted. For this design $S_w/A_t = 5.3$, and it is the most attractive design from a surface-area point of view.

Fan-face Mach Number - All the designs shown in figure 15 have a design fan-face Mach number of 0.6. If this value must be reduced, such as by engine throttle reduction, to match the engine thrust to airplane drag at cruise, the inlet design problem becomes more difficult. Three factors can contribute to a higher cruise fan-face Mach number:

(1) A low design value for the fan pressure ratio tends to give a match between takeoff and cruise thrust requirements at a high fan-face Mach number.

(2) The cruise altitude can be selected to give an airplane-drag-to-engine-thrust match at a high cruise fan-face Mach number.

(3) If the fan is designed with variable-pitch fan blades or with variable inlet guide vanes, as may be desirable for rapid thrust modulation for control during vertical takeoff and landing, these same variable devices can also be used to modulate the thrust at cruise to achieve the desired thrust at a high fan-face Mach number.

In general, by the appropriate selection of cruise Mach number, throat-to-fan area ratio, and fan-face Mach number a nacelle with a minimum (or low) surface area can be designed.

Nacelle Contour - The nacelle friction drag is a function of surface area and the friction forces per unit surface area. Reductions in surface area were just discussed. The local friction forces per unit area can be reduced by the choice of the nacelle contour. The solid lines of figure 16 show a conventional nacelle and the corresponding surface Mach number distribution and local skin friction coefficients. There is an early boundary-layer transition from

laminar to turbulent flow with correspondingly high turbulent friction coefficients. The dashed lines are for a nacelle contour with a Mach number distribution that was selected to maintain a longer laminar run and to give a more rapid diffusion in the turbulent region so as to reduce the turbulent skin friction coefficients. The modified contour gives a lower friction drag but has a lower contraction ratio. This lower contraction ratio is acceptable if the BLC or BLM schemes discussed earlier are applied in order to improve the internal flow at low speeds.

CONCLUDING REMARKS

The consequences of the present analysis, in terms of yielding shorter, thinner nacelles, are summarized in figure 17. The nacelle of figure 17(a) was designed without boundary-layer control or lip devices. To meet the high-angle-of-attack, low-speed requirements, the lower lip is very thick, a contraction ratio of 1.7. The upper lip was designed for good static performance with a contraction ratio of 1.3; the side lip has a contraction ratio of 1.5 to meet the crosswind requirements.

The nacelle of figure 17(b) meets the static and crosswind requirements with a lower contraction ratio, CR = 1.2, by using a lip slat. The high-angle-of-attack requirements on the lower lip are met with a retractable slat. This satisfies the conflicting requirements for a large lip frontal area at low speeds and a small frontal area at cruise.

The shorter diffuser is associated with the cruise design. The reduced length is possible because of the larger throat area and lower lip contraction ratio. The highlight areas of the two designs are essentially the same, so the additive drags are the same. The external frontal area of both nacelles was designed to generate the required leading-edge thrust.

In general, significant reductions in nacelle size can be achieved by optimum boundary-layer-managed or boundary-layer-controlled nacelle designs. The smaller nacelle because of its lower weight, the reduced bending moment on the engine frame, and the reduced cruise drag will increase the payload of V/STOL aircraft. A further consequence of these smaller nacelles is that the optimum fan pressure ratio for V/STOL Aircraft will tend to be lower, yielding further improvements in airplane performance.

REFERENCES

1. R. J. Shaw, R. C. Williams, and J. L. Koncsek, "V/STOL Tilt Nacelle Aerodynamics and Its Relation to Fan Blade Stresses," National Aeronautics and Space Administration TM-78899 (1978).

2. H. C. Potonides, R. A. Cea, and T. F. Nelson, "Design and Experimental Studies of a Type "A" V/STOL Inlet," AIAA, Paper 78-956, 1978.

3. J. A. Cawthon, "Design and Preliminary Evaluation of Inlet Concepts Selected for Maneuver Improvement," AIAA, Paper 76-701, 1976.

4. R. H. Liebeck, Design of Subsonic Airfoils for High Lift, Journal of Aircraft, Vol. 15, No. 9, pp. 547-561, September 1978.

5. A. M. O. Smith, High Lift Aerodynamics, Journal of Aircraft, Vol. 12, No. 6, pp. 501-530, June 1975.

6. M. A. Boles and N. O. Stockman, Use of Experimental Separation Limits in the Theoretical Design of V/STOL Inlets, Journal of Aircraft, Vol. 16, No. 1, pp. 29-34, January 1979.

7. R. W. Luidens, N. O. Stockman, and J. H. Diedrich, "An Approach to Optimum Subsonic Inlet Design," ASME, Paper 79-GT-51, 1979.

8. B. S. Stratford, The Maximum Pressure Rise Attainable in Subsonic Diffusion, Journal of the Royal Aeronautical Society, Vol. 67, pp. 275-278, April 1965.

9. J. A. Albers and B. A. Miller, "Effect of Subsonic Inlet Geometry on Predicted Surface and Flow Mach Number Distributions," National Aeronautics and Space Administration TN D-7446 (1973).

10. N. O. Stockman, Potential and Viscous Flow in VTOL, STOL, and CTOL Propulsion System Inlets, AIAA, Paper 75-1186, 1975.

11. B. A. Miller, A Novel Concept for Subsonic Inlet Boundary-Layer Control, Journal of Aircraft, Vol. 14, No. 4, pp. 403-404, April 1977.

12. B. A. Miller, B. J. Dastoli, and H. L. Wesoky, "Effect of Entry-Lip Design on Aerodynamics and Acoustics of High-Throat Mach-Number Inlets for the Quiet, Clean, Short-Haul Experimental Engine," National Aeronautics and Space Administration TM X-3222 (1975).

13. R. R. Burley, "Effect of Lip and Centerbody Geometry on Aerodynamic Performance of Inlets for Tilting-Nacelle VTOL Aircraft," AIAA, Paper 79-0381, 1979.

14. J. M. Abbott, "Aerodynamic Performance of Scarf Inlets," AIAA, Paper 79-0381, 1979.

15. R. R. Burley, A. L. Johns, and J. H. Diedrich, "Subsonic VTOL Inlet Experimental Results," In Proceedings of a Workshop on V/STOL Aircraft Aerodynamics, Naval Post Graduate School, Monterey, CA, May 16-18, 1979, Vol. II, pp. 648-664. Sponsored by Naval Air Development Center.

16. A. L. Johns, R. C. Williams, and H. C. Potonides, "Performance of a V/STOL Tilt-Nacelle Inlet with Blowing Boundary Layer Control," AIAA, Paper 79-1163, 1979.

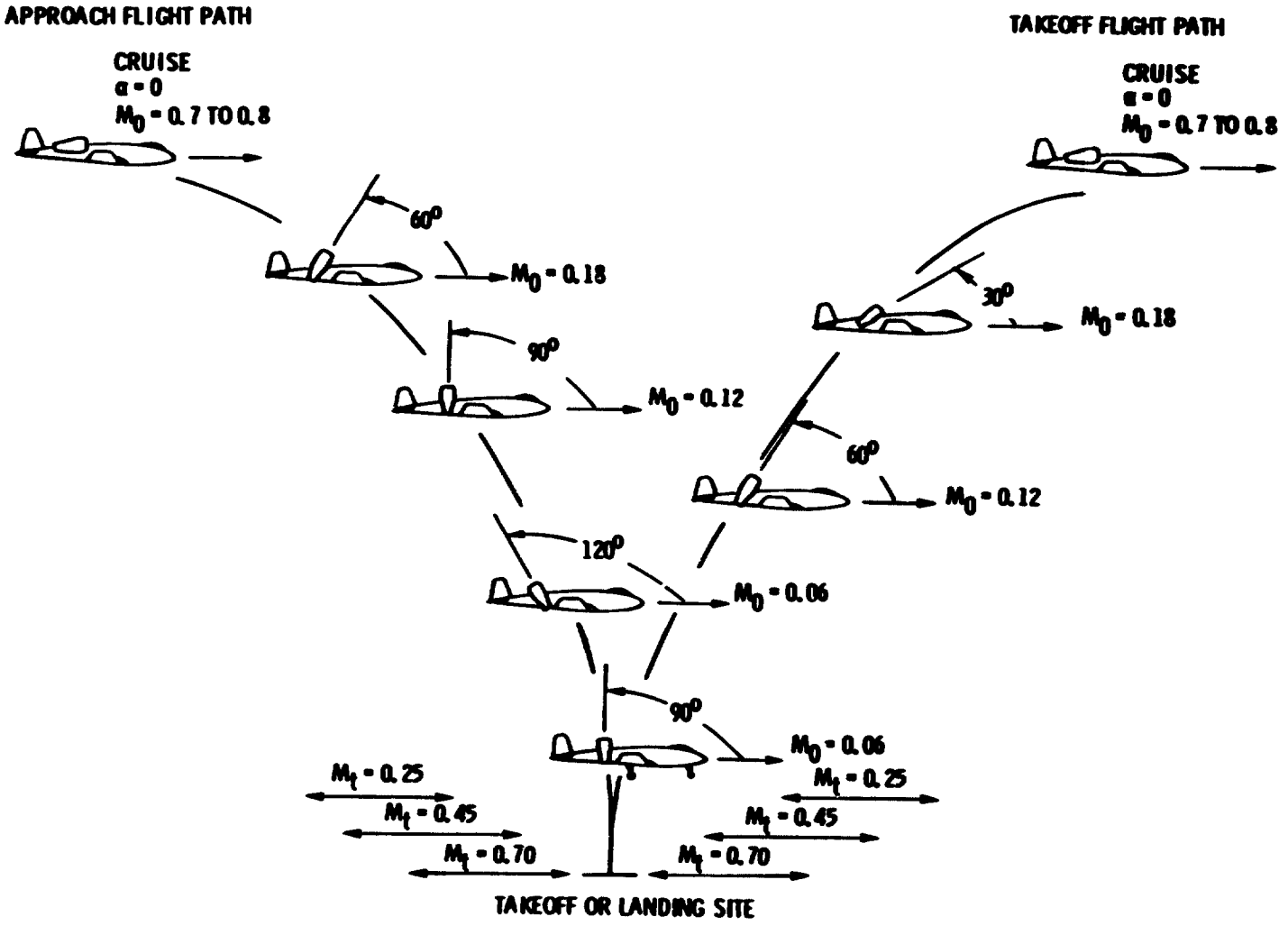

Figure 1. - Representative flight conditions for tilt-nacelle VTOL aircraft.

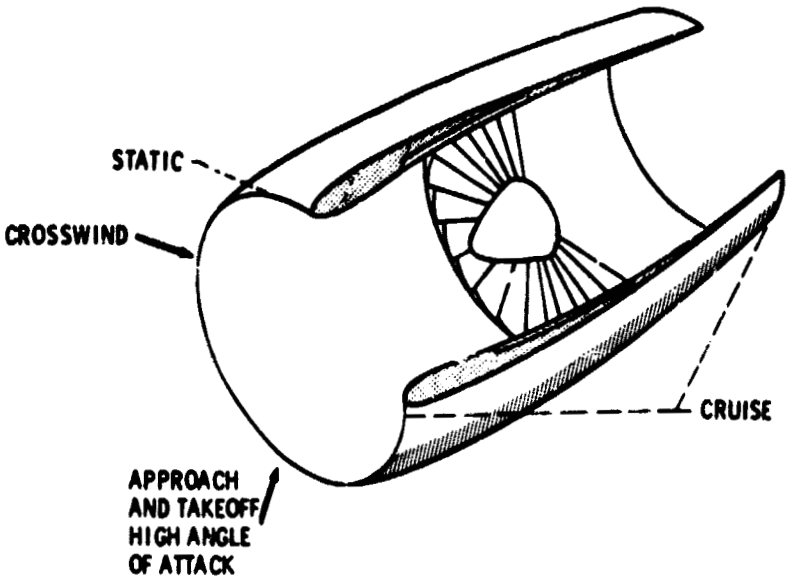

Figure 2. - Critical nacelle regions.

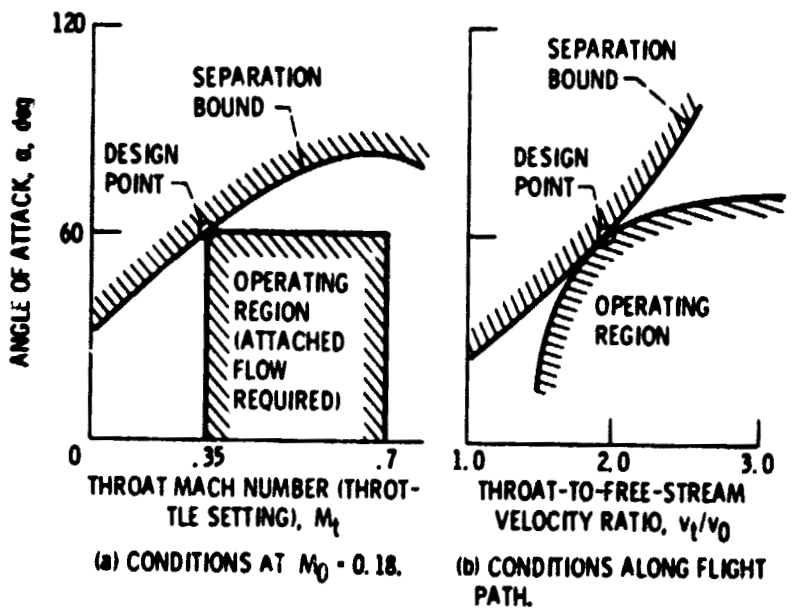

Figure 3. - Initial design-point selection.

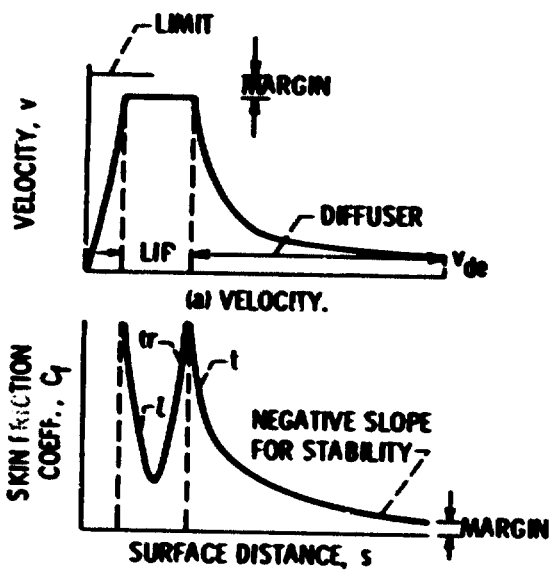

Figure 4. - Optimum flow distributions for inlets without boundary-layer control.

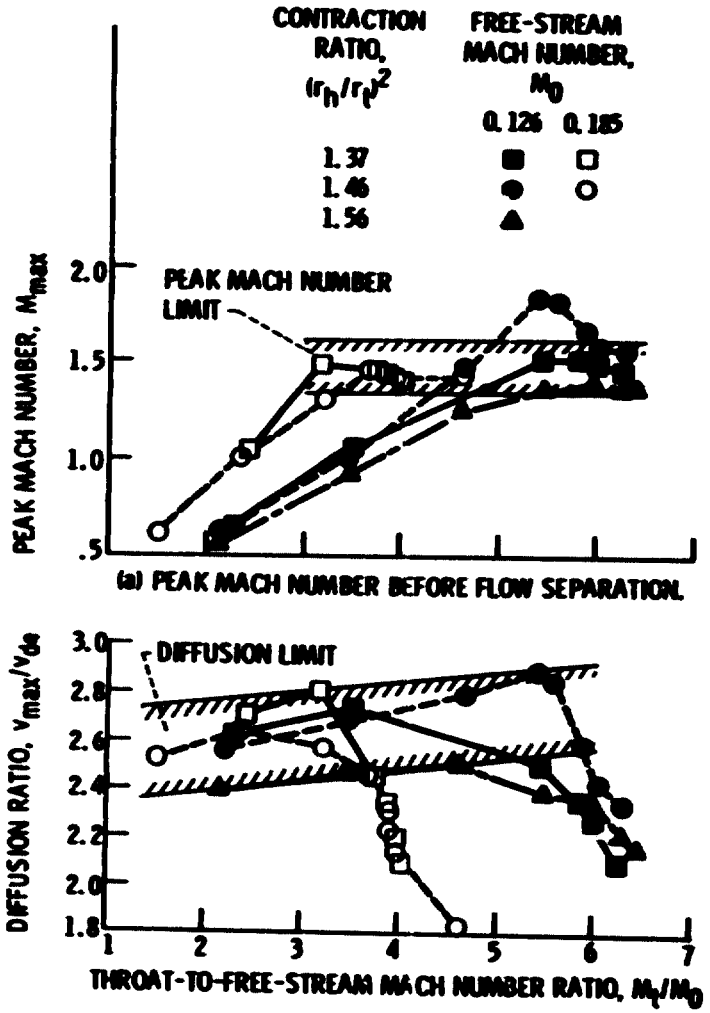

Figure 5. - Experimental separation data for inlets. (From ref. 6.)

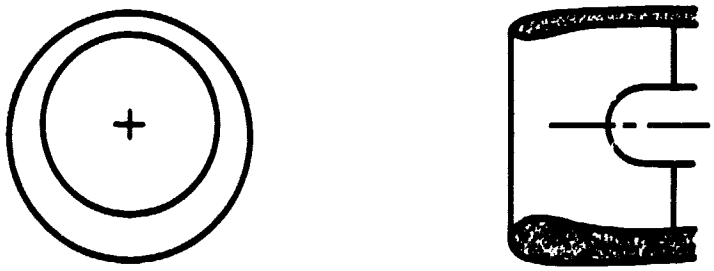

(a) THICK LOWER LIP.

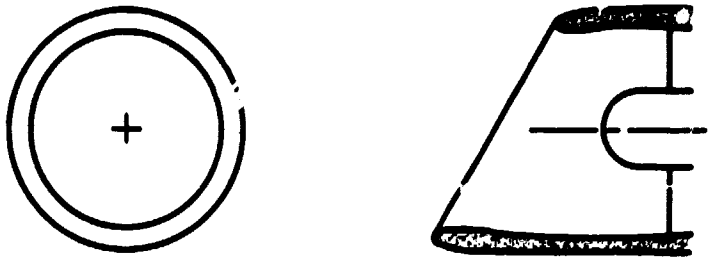

(b) PROTRUDING LOWER LIP.

Figure 6. - Low-speed, high-angle-of-attack inlets without boundary-layer control.

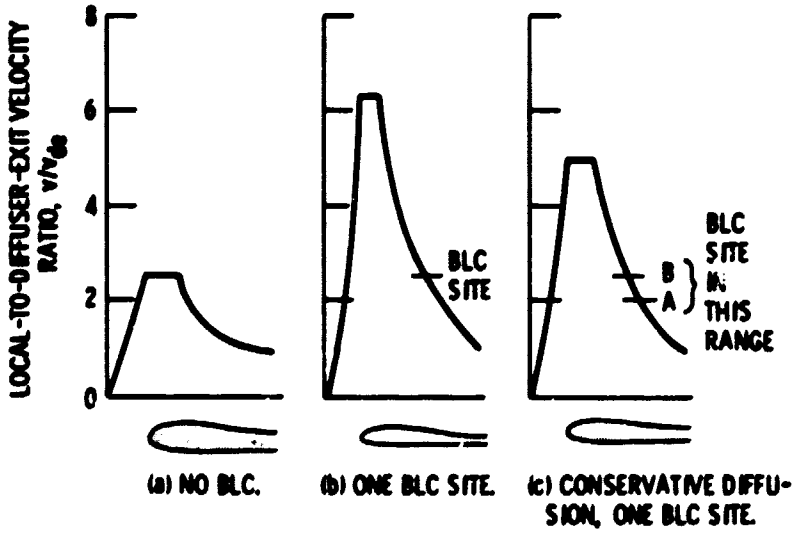

Figure 7. - Optimum inlet velocity distributions with boundary-layer control.

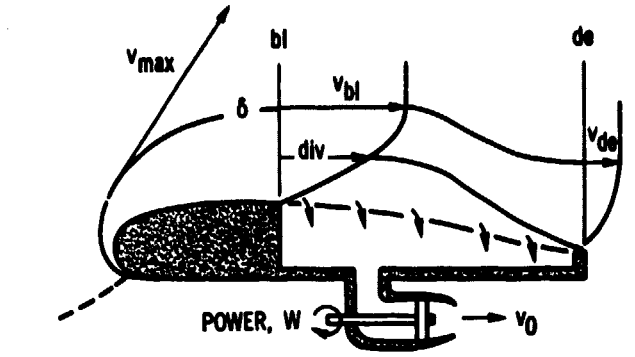

(a) SUCTION.

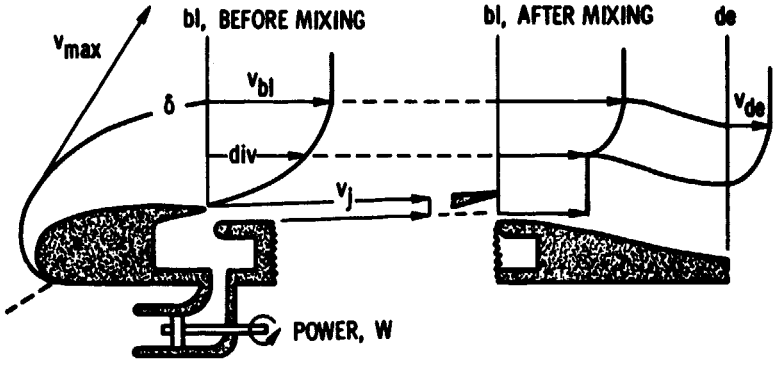

(b) BLOWING.

Figure 8. - Powered boundary-layer-control systems. (Boundary-layer heights exaggerated.)

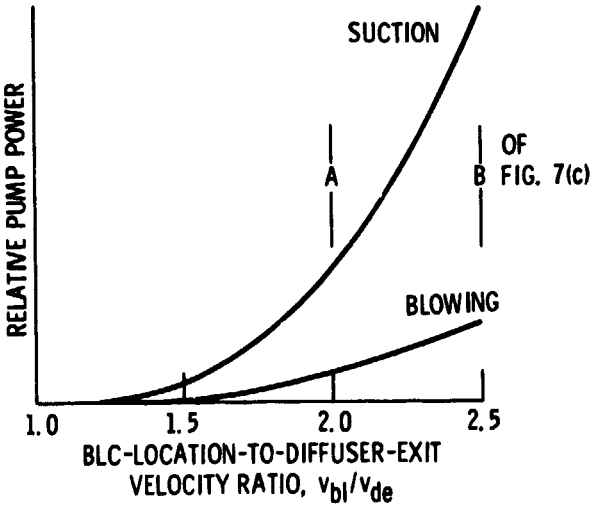

Figure 9. - Pumping power requirements for boundary-layer control. $v_{max}/v_{de} \leq 6.25$; $M_{de} = 0.3$; $v_j/v_{bl} = 2.0$; 1/7-power boundary-layer velocity profile.

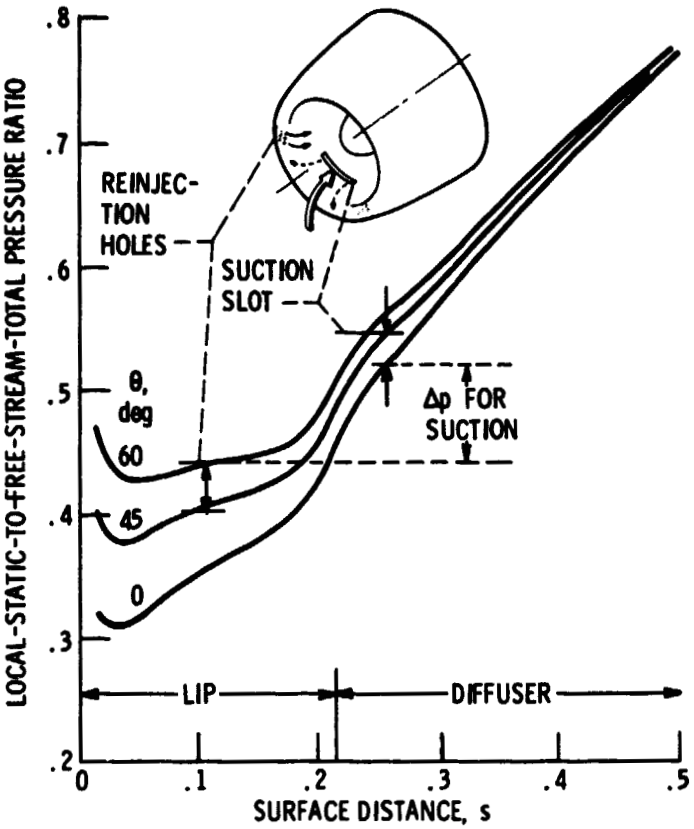

Figure 10. - Self-pumping boundary-layer-control system.

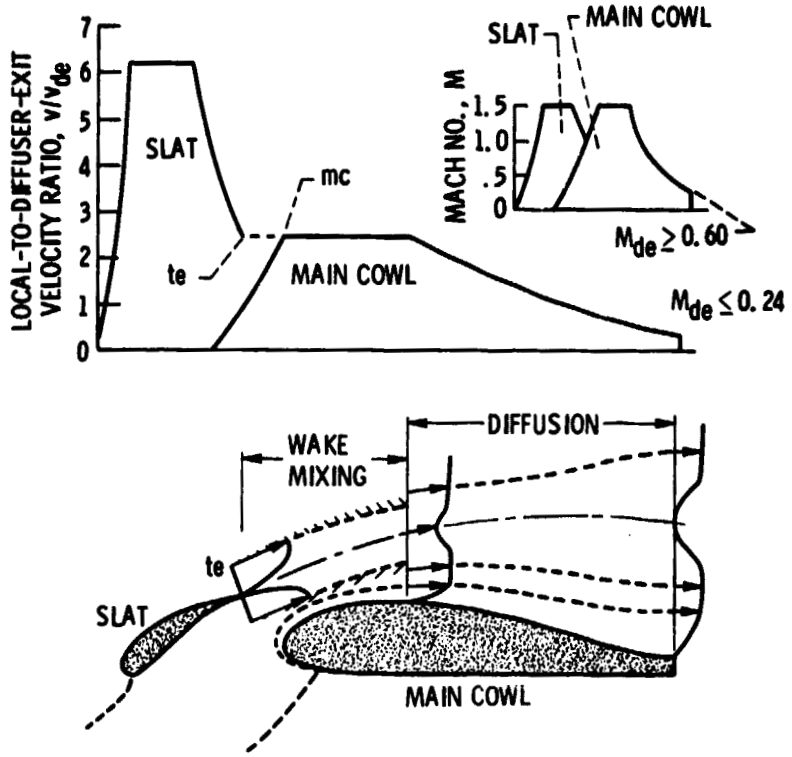

Figure 11. - Optimum inlet velocity distribution with boundary-layer management. (Boundary-layer heights exaggerated.)

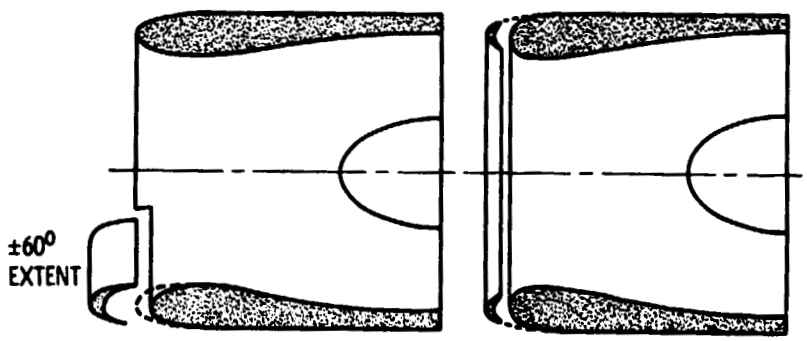

INCREASED CONTRACTION RATIO
LOWER LIP PROTRUSION
MECHANICAL ACTUATION

(a) INLET WITH RETRACTABLE SLAT.

INCREASED INFLOW AREA
INCREASED SURFACE AREA
SELF ACTIVATING

(b) SLOTTED INLET.

Figure 12. - Inlets with boundary-layer management.

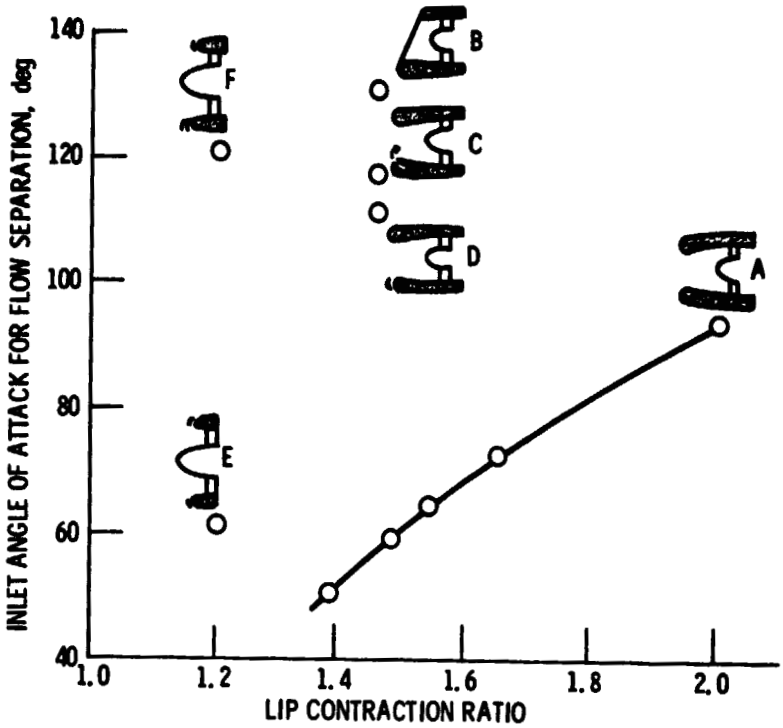

Figure 13. - Summary of experimental results for high-angle-of-attack inlets. $M_0 = 0.13$; $M_t = 0.45$.

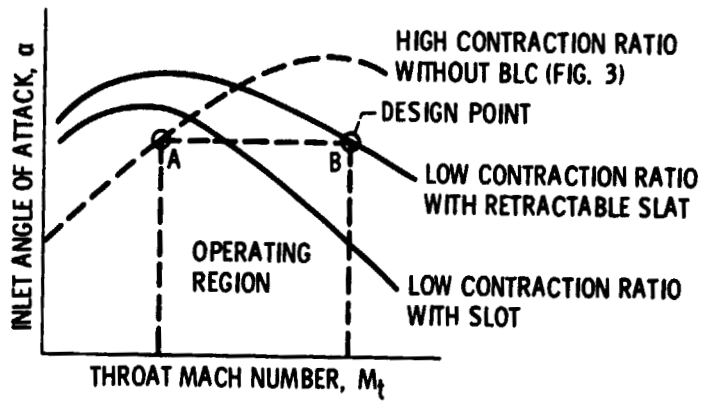

Figure 14. - Review of inlet design-point selection.

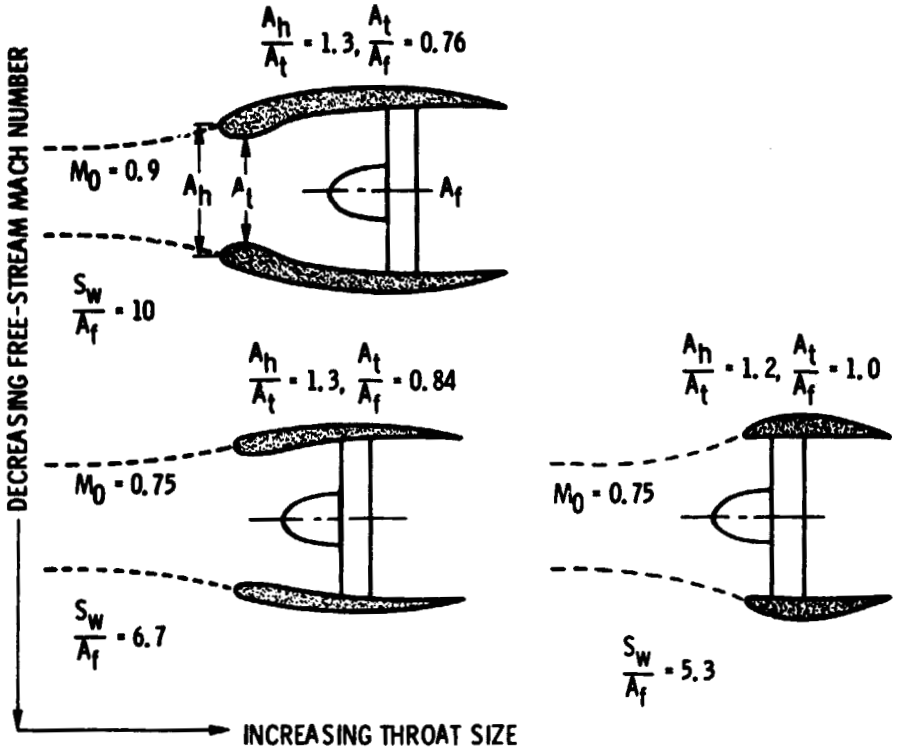

Figure 15. - Effect of free-stream Mach number and inlet throat size on nacelle wetted area.

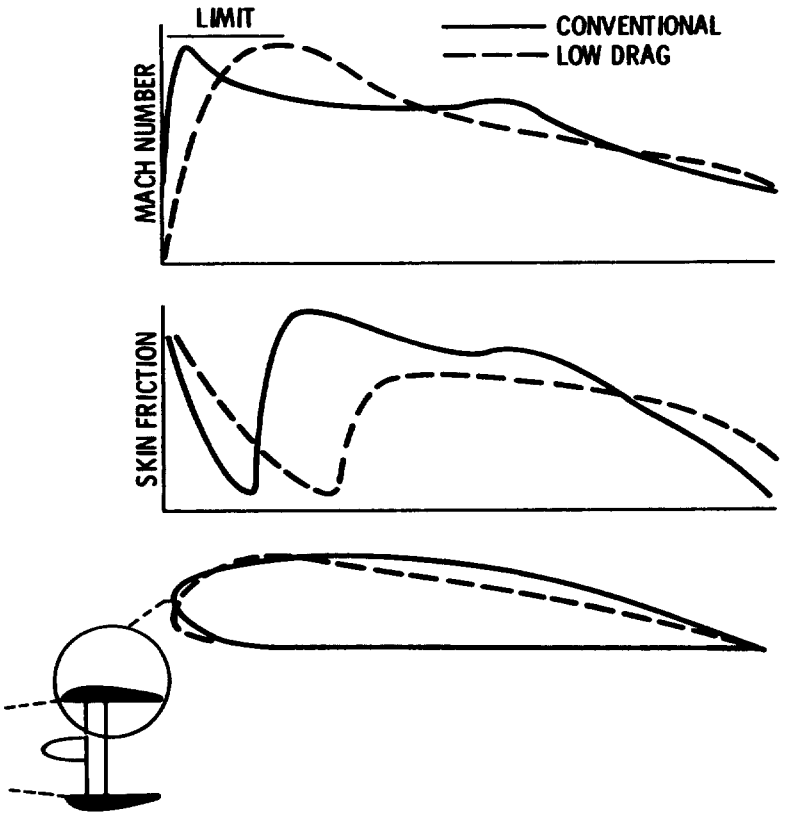

Figure 16. - Nacelle profile for low drag.

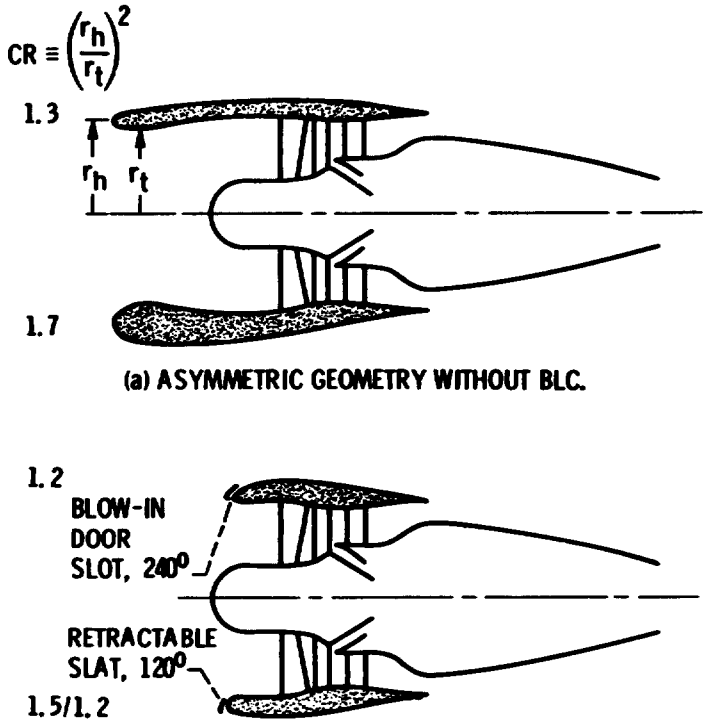

Figure 17. - Comparison of subsonic high-angle-of-attack nacelles.